Advanced Composite Materials
Publication details, including instructions for authors and subscription information:
http://www.tandfonline.com/loi/tacm20

A stress analysis of a mechanical joint for carbon composite rods

K.S. Kim [a] & H.T. Hahn [b]

[a] Advanced Composites Center, Daewoo Heavy Industries, Ltd., Changwon, Korea

[b] Mechanical, Aerospace and Nuclear Engineering Dept., University of California, Los Angeles, California 90024, USA

Version of record first published: 02 Apr 2012.

To cite this article: K.S. Kim & H.T. Hahn (1998): A stress analysis of a mechanical joint for carbon composite rods, Advanced Composite Materials, 7:2, 137-150

To link to this article: http://dx.doi.org/10.1163/156855198X00101

Adv. Composite Mater., Vol. 7, No. 2, pp. 137–150 (1998)

A stress analysis of a mechanical joint for carbon composite rods

K. S. KIM[1,*] and H. T. HAHN[2]

[1]*Advanced Composites Center, Daewoo Heavy Industries, Ltd., Changwon, Korea*
[2]*Mechanical, Aerospace and Nuclear Engineering Dept., University of California, Los Angeles, California 90024, USA*

Received 25 November 1996; accepted 8 September 1997

Abstract—The high axial tensile strength and the low transverse strength of pultruded composite rods present some unique problems in testing with conventional grips. The high transverse compressive forces required in the conventional method of gripping tent to crush the rod, thereby causing premature failure. Design guidelines for an end tab grip adapter used in tensile testing of pultruded composite rods can be found in ASTM standard D3916-84. Although this standard is applicable to glass fiber reinforced rods, it is inadequate for high-strength composites because of slip. It is therefore necessary to develop and characterize a new tension jig for high-strength fiber composite rods such as graphite fiber composites. The present paper presents results from a two-dimensional nonlinear finite element analysis to characterize the contact pressure and stress distributions at the interfaces and maximum axial load available in the jig developed.

Keywords: Carbon composite rod; tensile strength; tension jig; transverse strength; contact stress.

1. INTRODUCTION

The anisotropic and brittle nature of high strength unidirectional pultruded composites make tensile testing very difficult because of premature failure with the conventional gripping method [1]. In order to alleviate the load introduction problem the typical tension and compression specimen has tabs bonded to specimen ends. A finite element analysis of a tension coupon specimen with tapered tab geometry was reported in conjunction with the wedge-action grip mechanism of the testing machine [2]. Results of this study indicate that stresses are generally lower with tapered tab geometry. Peak stresses at the end of the tab are found to be sensitive to tab length, thickness, and layer orientation, as well as the stiffness of the test laminate. Rizzo and Vicario [3] performed a finite element analysis to determine the stress distribution in gripped tubular specimens. For a tube under uniform axial extension, axial stress concentration under the grip was found to be as high as 140 percent of the average

*To whom correspondence should be addressed.

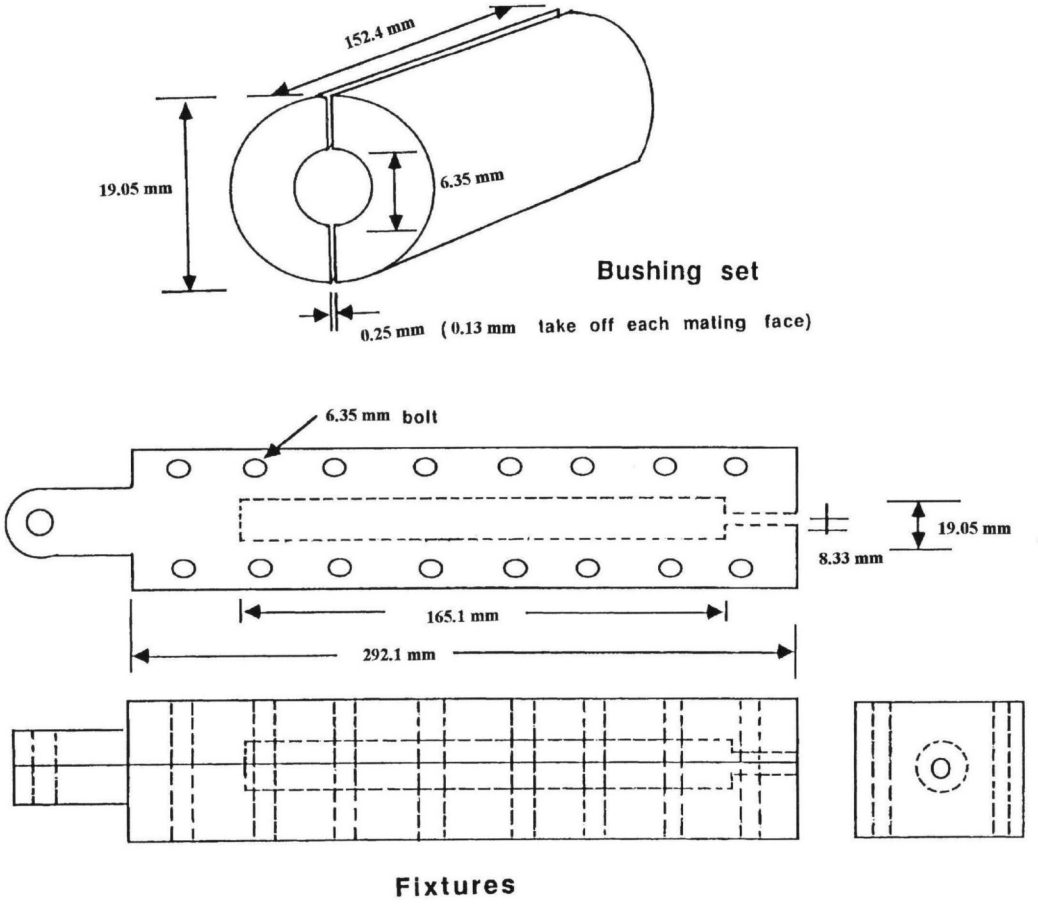

Figure 1. Tension jig for pultruded composite rod.

applied stress. However, this model did not include load transition schemes such as end tabs. Whitney *et al.* [4] investigated the effect of end moments and load introduction on the strength of a composite cylinder using Flugge's shell theory with failure criterion. It was found that stress concentration in the end tab could be substantially relieved by relaxing the end-clamping condition.

Design guidelines for end tab grip adapters in tensile testing of pultruded composite rods can be found in ASTM standard D3916-84. These guidelines, however, are not applicable to high strength fiber reinforced composite rods because of slip as a result of higher failure load required.

A new frictional jig was designed as shown in Fig. 1. In order to determine the ultimate tensile strength, the bolt-clamping forces and resultant contact pressure between the specimen and the tab should be adequate to prevent pullout of the specimen as well as premature failure at the critical regions. The premature failure due to stress concentration at the end of the tab can be eliminated by controlling the slip through the change of bolt-clamping forces and friction coefficient along the interface. It is therefore necessary to characterize the interfacial contact stresses in a new tension jig.

In the present study, a two-dimensional nonlinear analysis was performed to determine the contact stress distribution around and along the specimen under the tab and also the maximum axial load possible in jig. Emphasis was on delineating the effect of friction coefficient, material properties of the tab, and slip between the tab and the specimen on the interfacial contact stress distribution. The results would be helpful also in designing mechanical joints for ropes such as tethers for a tension leg platform [5].

2. ANALYSIS

In testing circular pultruded rods, the specimen is placed between two cylindrical bushings, called tabs hereafter, and two steel fixtures are bolted together to apply pressure on the specimen as shown in Fig. 1. The steel fixtures are joined by several bolts evenly spaced. The bolts are tightened to a certain preload. During tensile testing, the axial force applied to the steel fixtures is transmitted to the specimen through the friction at the specimen/tab interface. Good gripping of the specimen in the jig is ensured by the condition;

$$F_f \geqslant F_X^{max}/2, \tag{1}$$

where F_X^{max} is the maximum axial load to be applied and F_f is the friction force between the specimen and one of the tabs.

The friction force is determined by

$$F_f = f p_c A_i, \tag{2}$$

where f is the friction coefficient, p_c is the average contact pressure, and A_i is the contact surface area between the specimen and the steel tab. Since the friction

Table 1.
Material property and geometry data used

Fixture & bushing:	
steel	$E_s = 207$ GPa, $\nu_s = 0.3$
aluminum	$E_a = 69$ GPa, $\nu_a = 0.3$
Specimen: Gr/PPS*	$E_{11} = 120.6$ GPa
	$E_{22} = E_{33} = 8.6$ GPa
	$G_{12} = G_{23} = G_{31} = 4.2$ GPa
	$\nu_{12} = \nu_{23} = \nu_{31} = 0.36$
	$X_t = 1378$ MPa, $X_c = 861$ MPa
	$Y_t = 35$ MPa, $Y_c = 138$ MPa
	$S = 69$ MPa
Friction coefficient	$f = 0.2$
Geometry data:	Specimen diameter = 6.35 mm
	Gap size = 0.25 mm
	Tab diameter = 9.53 mm
	Tab length = 15.24 mm

*From private communication with manufacturer.

coefficient of unidirectional graphite/epoxy composite against a smooth steel surface is around 0.2 in the fiber direction [6], f is assumed to be 0.2 in this analysis. The same friction coefficient was applied to the contact surface between the tab and the steel fixture.

It is now desirable to find the bolt tension that must be applied to prevent slip without causing premature failure of the specimen. The average contact pressure can be determined from the static equilibrium condition. Twice the applied pressure will be induced at the tab/specimen interface based on input data (Table 1). From the above equations, the applied pressure should be higher than 41.3 MPa to prevent slip. By using the stress output in conjunction with the failure criterion [7], the maximum value of applied pressure will be determined.

For simplicity of analysis, the problem was divided into two parts as follows.

2.1. Around the specimen

Since the bolt hole size was not an important parameter for the contact stress distribution, it was not included in the analysis. The discrete bolt forces along the outer steel fixture were replaced by a continuous loading. Since the specimen length was much longer than its diameter, stress analysis was performed under the assumption of plane strain. The bolts were tightened to apply a compressive pressure (p_b) of, for example, 68.9 MPa. Because of the symmetry, only one quarter of the cross-section was analyzed (Fig. 2).

The stress analysis was performed using the ANSYS finite element code [8]. Three sets of elements were used to model the assembly. Two-dimensional 3-node and 4-node isoparametric elements were used for the solid body. A typical layout of elements and boundary conditions is shown in Fig. 3 (180 elements and 180 nodes). At the two different interfaces, double nodes with identical nodal coordinates were

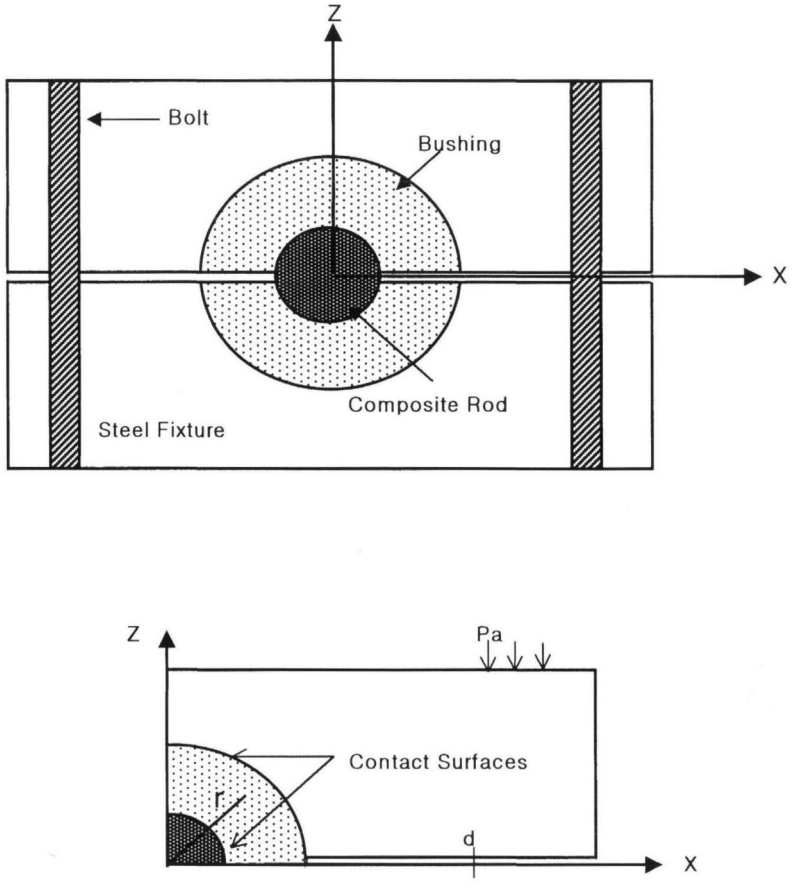

Figure 2. Typical cross-section of tension jig.

used. A two-dimensional nonlinear gap element [8] was applied to connect these two nodes. This element is defined by two nodal points, an interface stiffness (k), an initial gap (or interference), and an initial element status. The interface stiffness should be based on the stiffness of the surface in contact [9]. Since the local surface deformation is not of importance, k may be estimated as an order of magnitude of the adjacent element stiffness:

$$k = A_e E/L, \tag{3}$$

where A_e is equivalent nodal area; E is the modulus of adjacent material; and L is arbitrary element length.

Trial runs showed that the contact stress distribution is nearly independent of the stiffness (k). Therefore, L was arbitrarily assumed as $1/10$ of the adjacent element height, 0.025 mm. Equivalent nodal area, A_e, was determined by multiplying the average length and thickness of adjacent elements to the nodal point. E was taken to be the modulus of steel for both contact surfaces. The force–deflection relationships for the interface element are considered separately in the normal and tangential (sliding) directions.

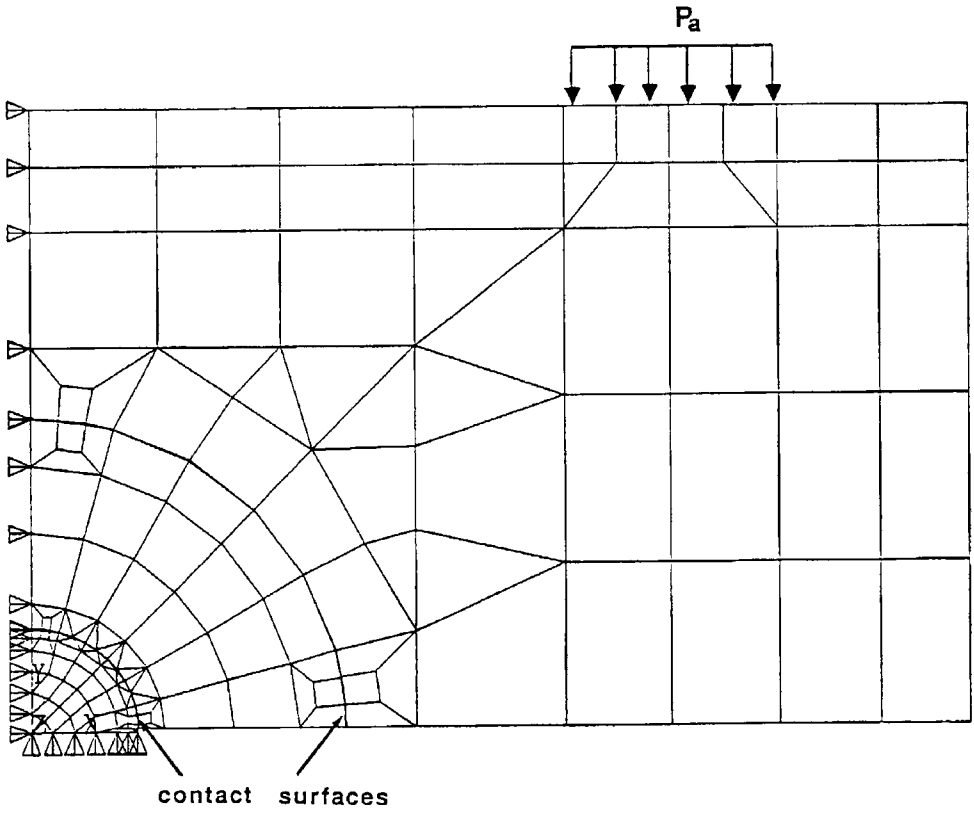

Figure 3. Element and node layout for finite element analysis.

In the normal direction, when the normal force (F_n) is negative, the interface remains in contact and responds as a linear spring. As the normal force becomes positive, contact is broken and no force is transmitted. In the tangential direction, if $F_n < 0$ and the absolute value of the tangential force (F_S) is less than or equal to $f|F_n|$, the interface does not slide and respond as a linear spring. However, if $F_n < 0$ and $F_S > f|F_n|$, sliding occurs. If contact is broken, no tangential force is required to produce sliding. This element is nonlinear and requires an iterative procedure, with the stiffness matrix reformulated for each iteration, for static convergence. The condition for convergence was the friction force being less than 10 percent different between any successive iteration.

The purpose of this analysis was to delineate the effect of the friction coefficient and material property of the tab on the contact pressure and interfacial stress distributions, and to provide information for the design of slip-proof joint.

2.2. *Along the specimen*

Since the contact pressures at the tab/fixture and tab/specimen interfaces were found to be nearly uniform except at the gaps in the preceding section, the real 3-dimensional problem was simplified to a two-dimensional axisymmetric problem. The modified

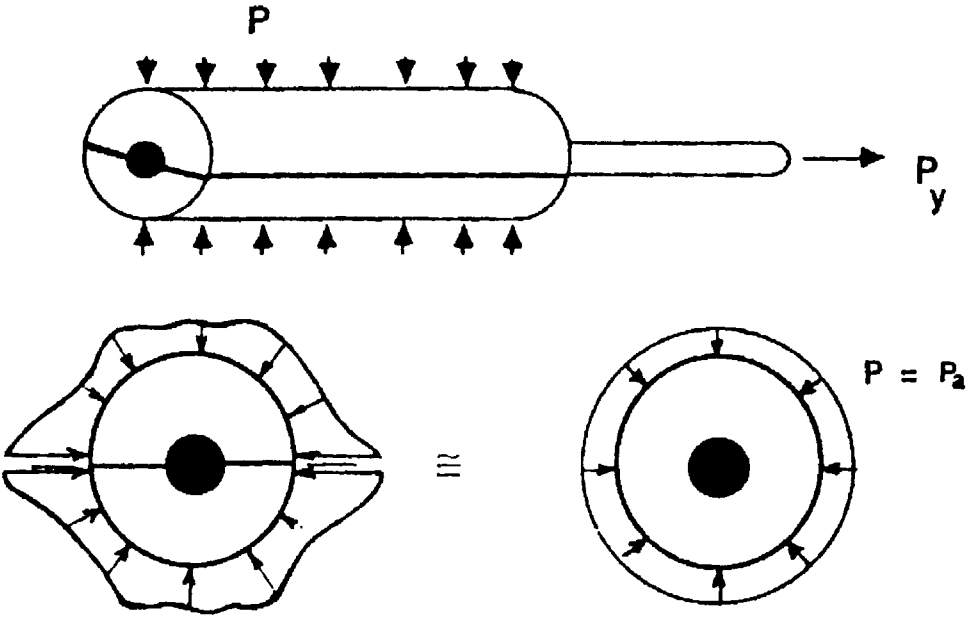

Figure 4. Simplified model for the analysis of axial loading.

problem thus consisted of a cylindrical composite rod surrounded by a cylindrical metal tab with a uniform pressure applied at the outer boundary as shown in Fig. 4.

The question was to find the contact pressure distribution, the slip condition and its effect on the stress distribution, and maximum axial load that can be applied without total slip. In the longitudinal direction, we have used axisymmetric 4-node isoparametric elements. From the symmetry about the mid-plane, only one half of the assembly was considered. Also, the same gap elements as described earlier were used to simulate the interface between the tab and the composite rod. The boundary conditions and element layout are shown in Fig. 5.

3. RESULTS AND DISCUSSION

The material properties and geometry data used in the analyses are listed in Table 1. All the results are normalized by either the bolt-clamping pressure or the applied axial stress.

The contact pressure distributions at the tab/fixture interface are shown in Fig. 6. The effect of friction is seen to increase the contact pressure over most of the interface. Also, the contact pressure is nearly uniform except at the junction ($\theta = 90°$) and its areal average is equal to the applied pressure, because the tab and bolt have the same cross-sectional area.

Figure 7 shows the contact pressure distribution at the tab/composite interface. Although there is a significant pressure concentration at the gap, it is interesting to see a nearly uniform pressure distribution over most of the interface. Contrary to

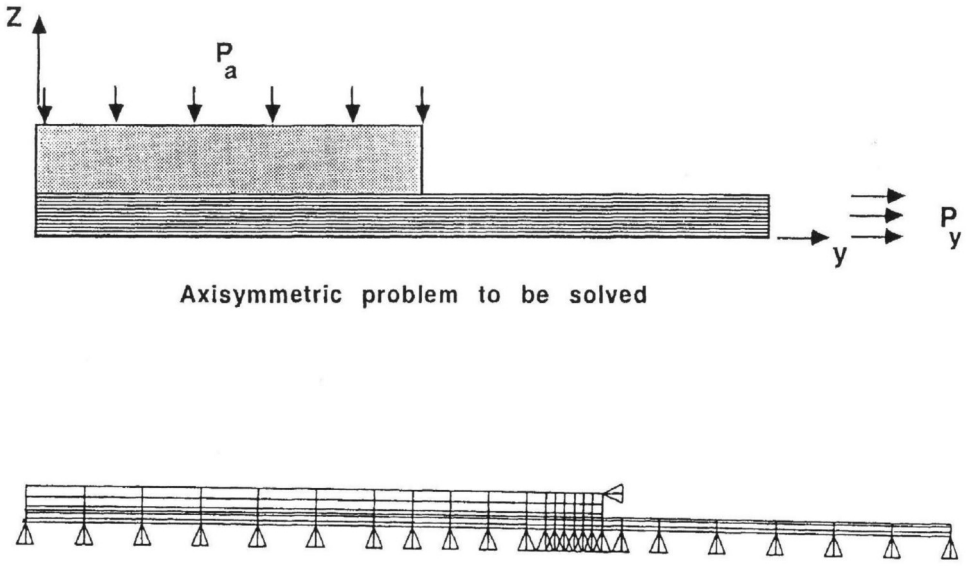

Figure 5. Element and node layout for finite element analysis.

Fig. 6, the frictionless surface causes slightly higher contact pressure over the major portion of the interface. The average value is, however, independent of friction and is nearly equal to $2P_a$, because the ratio of cross-sectional area between the bolt and the specimen is 2.

A steel tab was also analyzed to see its effect on the contact pressure distributions. Since there was little difference, however, the results are not shown. The radial and tangential stress distributions in the composite rod near the interface are shown in Figs 8 and 9. These stresses were normalized by the bolt pressure. Interestingly, stresses are quite uniformly distributed. Such uniform stress distributions are needed to prevent premature failure. The limiting case of infinite friction coefficient, perfectly bonded interface, was considered by eliminating the gap element and imposing a continuity condition at the interface. As the friction coefficient increases, the radial stress decreases, like contact pressure. However, this trend is reversed near the junction for tangential stress. Also, a significant shear stress concentration is observed at the same point. These results indicate that the bonded tab may debond due to a high shear stress concentration [1].

Equivalent stress [10] contours with a friction coefficient of 0.2 are shown in Fig. 10. The maximum value is seen to exist at the junction as expected. Therefore, the bolt pressure should be adjusted so as not to cause premature failure at this point. The calculated stresses were used in the Tsai–Hill failure criterion [7] to determine the maximum bolt pressure that could be applied without failure of the composite rod. It was found that there was no failure in the specimen until the bolt pressure was increased to 75.8 MPa.

The axial distribution of the contact pressure at the tab/specimen interface was found by using the two-dimensional axisymmetric finite element model, as shown in

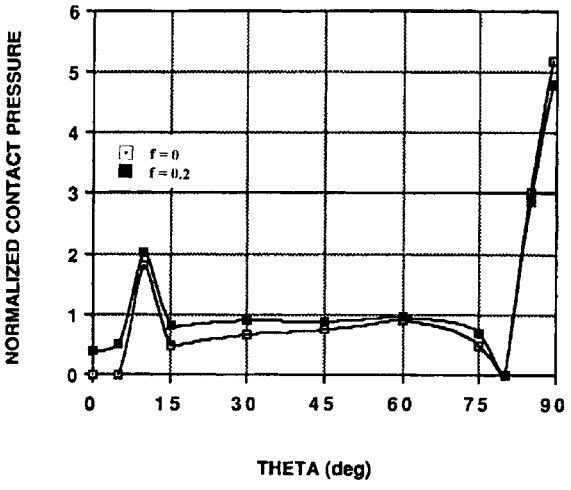

Figure 6. Normalized contact pressure distribution at the interface between steel tab and fixture.

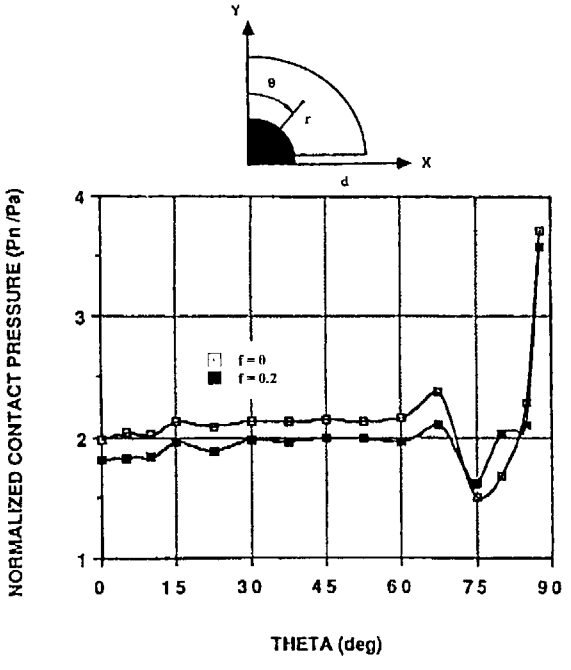

Figure 7. Normalized contact pressure distribution at the interface between steel tab and specimen.

Fig. 5. Here, the uniform pressure applied on the tab boundary is the areal average of the tab/fixture contact pressure determined in Fig. 6.

Figure 11 shows the change of the contact pressure as the applied axial load increases. As the axial load increases, slip starts at the tab end and grows inward, as shown in Fig. 12. The pressure concentration seems to decrease as the slip area increases.

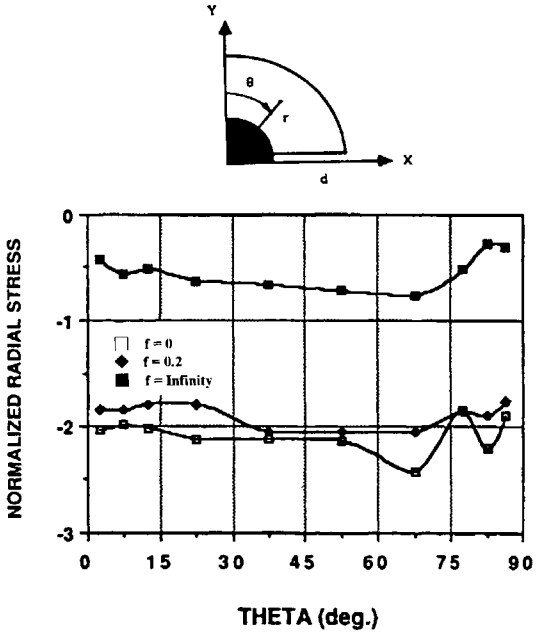

Figure 8. Normalized radial stress, σ_r, distribution in the specimen near the interface (at $r/r_0 = 0.96$).

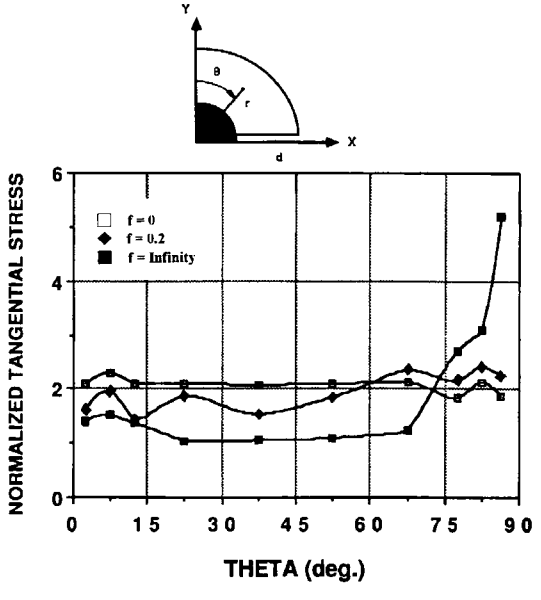

Figure 9. Normalized tangential stress, σ_θ, distribution in the specimen near the interface (at $r/r_0 = 0.96$).

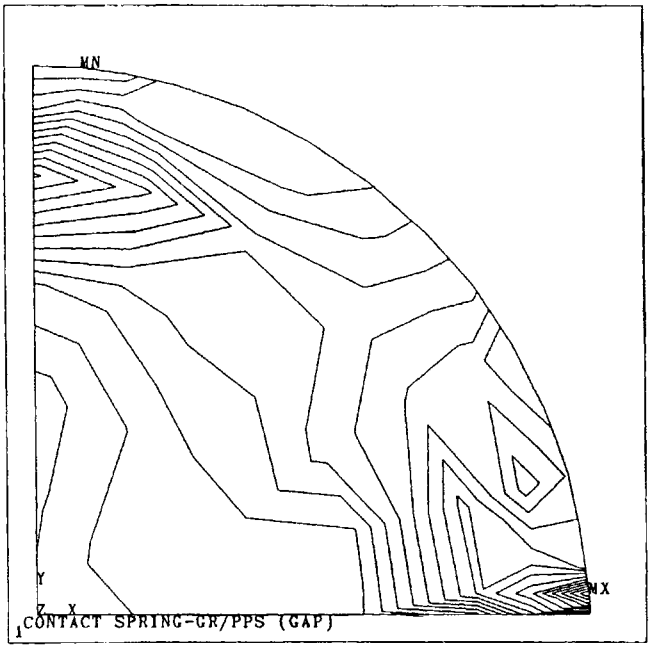

Figure 10. Equivalent stress contours in the specimen.

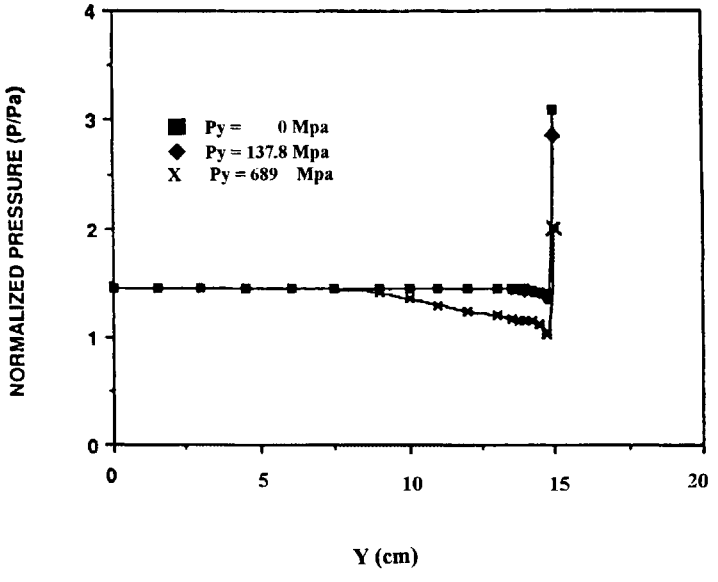

Figure 11. Normalized contact pressure distribution at the interface between specimen and tab.

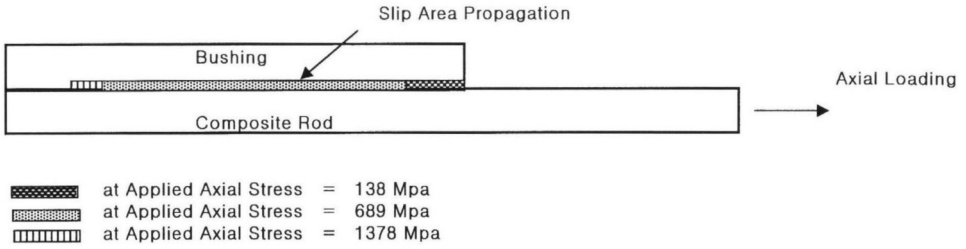

Figure 12. The slip area according to the applied axial stress.

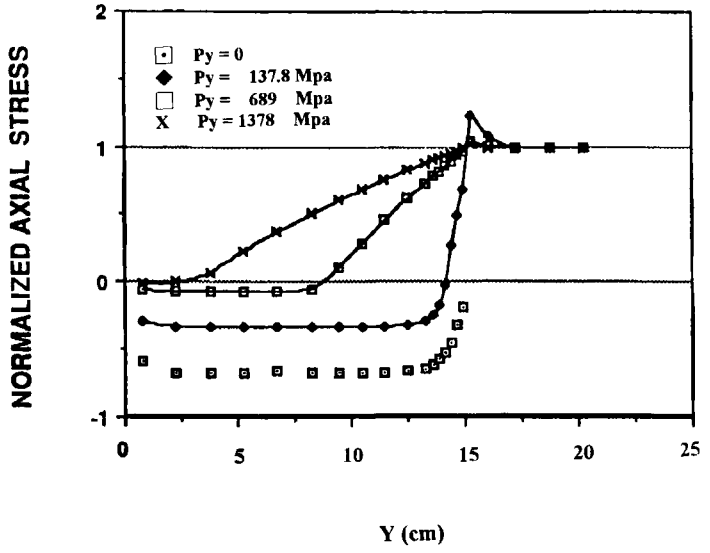

Figure 13. Normalized axial stress, σ_y, distribution near the interface (at $r/r_0 = 0.9$).

However, it should be noted that the average contact pressure at the tab/specimen interface is about 30 percent lower, or 48.2 MPa, than the average pressure of Fig. 7. Since the gap between the tabs, d, was neglected in the analysis of Fig. 11, the resulting pressure was lower. Under the bolt pressure of 68.9 MPa, the specimen is expected to be pulled out when an axial stress of 1378 MPa, which is about failure strength of the specimen, is applied. From an additional computer run, it was found that the specimen pullout could be prevented by increasing the bolt pressure about 5 percent. Under the increased bolt pressure, the slip area was about 86 percent of the total contact area (Fig. 12). When the gap d is allowed, the required bolt pressure is expected to be about 51.7 MPa, rather than the 72.3 MPa determined earlier without the gap. It is interesting to note that this value is close to the bolt pressure of 41.3 MPa, which is estimated from simple static equilibrium conditions (equations (1) and (2)).

The axial stresses distribution near the interface, normalized by the applied axial stress, are shown in Fig. 13. When there is little slip between the specimen and the tab, stress concentration can be as high as 125 percent at the end of tab. As

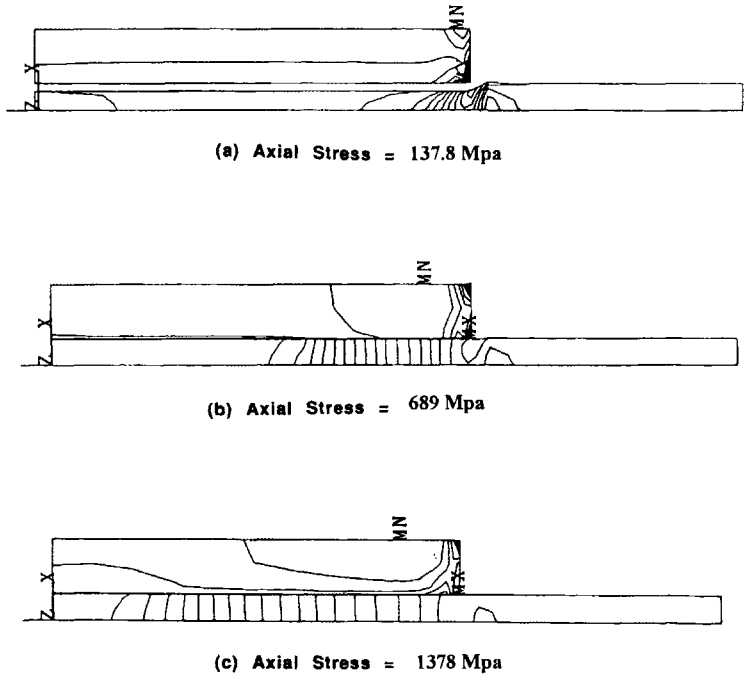

Figure 14. Equivalent stress contours for several loading cases. (a) $p_y = 138$ MPa; (b) $p_y = 689$ MPa and (c) $p_y = 1378$ MPa (deformation is 3 times magnified in the radial direction).

the applied axial load increases, the slip area increases, and the stress concentration decreases and finally disappears. Therefore, the stress concentration will not cause premature failure during tensile testing. Also, the bolt pressure around 55.1 MPa will be enough to allow the tensile strength of graphite/PPS, which is 1378 MPa, to be measured without total slip.

Another interesting point is that as slip propagates inward, a large portion of the specimen under the tab becomes effective in supporting the axial load (Fig. 14). Also, the stress concentration at the tab end is substantially reduced.

4. CONCLUSIONS

A finite element stress analysis was performed for a tension jig for composite rod. In particular, the effects of friction coefficient and slip on the contact pressure and axial stress distributions was studied. It was found that the contact pressure distribution around the specimen was quite uniform and nearly independent of the friction coefficient. The slip along the tab was found beneficial in relieving the axial stress concentration. These results would be helpful in designing slip-proof mechanical joints for composite rods. Other parameters like the nonuniform bolt clamping pressure and variable friction coefficient along the interface, and tab geometry such as tab shape and taper angle can be considered to minimize the stress concentration for the optimum design.

REFERENCES

1. Wronski, A. S. and Parry, T. V. Transverse (interlaminar) cracking under tensile loading pultruded CFRP. *J. Mater. Sci.* **19**, 3421–3429 (1984).
2. Kural, M. H. and Flaggs, D. L. A finite element analysis of composite tension specimens. *Compos. Technol. Rev.* **5** (1), 11–19 (1983).
3. Rizzo, R. R. and Vicario, A. A. A finite element analysis for stress distribution in gripped turbular specimens. In: *Composite Materials: Testing and Design (Second Conference), ASTM STP 497*. Am. Soc. for Testing and Mater. (1972), pp. 68–88.
4. Whitney, J. M., Grimes, G. C. and Francis, P. H. The effect of end attachment on the strength of fiber-reinforced composite cylinders. *Experimental Mechanics* **13** (5), 185–192 (1973).
5. Kim, K. S. and Hahn, H. T. A stress analysis of mechanical joint for advanced composites rods. *Daewoo Technology* **11** (2), 78–85 (1992).
6. Kim, K. S., Hahn, H. T. and Williams, J. G. Application of composites in TLP tethers. In: *Proc. 7th Intern. Conf. on Offshore Mechanics and Arctic Engineering*, Vol. III. OMAE, Houston, TX (1988), pp. 1–7.
7. Tsukizoe, T. and Ohmae, N. Friction and wear performance of unidirectionally oriented glass, carbon, aramid and stainless steel fiber-reinforced plastics. In: *Friction and Wear of Polymer Composites, Composite Material Series*, Friedrich, K. (Ed.), Vol. 1. Elsevier (1986), pp. 205–231.
8. Tsai, S. W. and Hahn, H. T. *Introduction to Composite Materials*. Technomic Publishing Company, Lancaster, PA (1980).
9. Swanson Analysis System, Inc. *ANSYS Engineering Analysis System Users Manual*, Vol. 1–2 (1993).
10. Leal, A. V. and Hinduja, S. Modelling the characteristics of interface surfaces by the finite element method. *Proc. Inst. Mech. Eng.* **198C** (4), 9–23 (1984).
11. Timoshenko, S. *Strength of Materials: Advanced Theory and Problems*. Robert E. Krieger, FL (1983).